Cell, Vol. 78, 603–615, August 26, 1994, Copyright © 1994 by Cell Press

The DNA Binding Specificity of Ultrabithorax Is Modulated by Cooperative Interactions with Extradenticle, Another Homeoprotein

Siu-Kwong Chan,* Leah Jaffe,* Maria Capovilla,‡ Juan Botas,† and Richard S. Mann*†
*Department of Biochemistry and Molecular Biophysics
†Center for Neurobiology and Behavior
Columbia University
New York, New York 10032
‡Institute for Molecular Genetics
Baylor College of Medicine
Houston, Texas 77030

Summary

The *Ultrabithorax* (*Ubx*) and *Antennapedia* (*Antp*) genes of Drosophila encode homeodomain proteins that have very similar DNA binding specificities in vitro but specify the development of different segmental patterns in vivo. We describe cooperative interactions between Ubx protein and a divergent homeodomain protein, extradenticle (exd), that selectively increases the affinity of Ubx, but not Antp, for a particular DNA target. We also provide evidence that Ubx and exd bind to neighboring sites on this DNA and interact directly to stabilize the DNA-bound form of Ubx. Thus, the ability of different homeotic genes to specify distinct segmental patterns may depend on cooperative interactions with proteins such as exd that selectively modulate their otherwise similar DNA binding specificities.

Introduction

Most animals have well-defined morphological differences along their anterior to posterior body axes. In insects, where the body plan is segmented, these differences are controlled by the homeotic genes that dictate the specific morphological characteristics of each segment (Lewis, 1978; Wakimoto and Kaufman, 1981). In Drosophila melanogaster, eight homeotic genes are clustered in the Antennapedia (Antp) and bithorax gene complexes and collectively constitute the homeotic complex or HOM-C (McGinnis and Krumlauf, 1992). Similar Homeotic Complexes have been identified in all higher eukaryotes that have been examined, and a significant body of evidence supports the idea that all HOM-C genes, such as the Drosophila homeotic genes, play important roles in regional pattern specification. Furthermore, all HOM-C genes encode homeodomain-containing proteins and, therefore, probably determine cell fates by binding to and regulating the transcription of downstream target genes (Andrew and Scott, 1992).

In contrast with their diverse in vivo functions, HOM-C proteins often bind to the same DNA sequences in vitro, indicating that their intrinsic DNA binding specificities are very similar (see Hoey and Levine, 1988; Desplan et al., 1988; reviewed by Treisman et al., 1992). An important problem, therefore, is how HOM-C proteins direct the development of distinct patterns. One possibility is that subtle differences in their in vitro DNA binding affinities are important in vivo. Indeed, quantitative differences in the DNA binding of HOM-C proteins exist and are likely to be important for distinguishing between some of their in vivo functions (Dessain et al., 1992; Ekker et al., 1992; Lin and McGinnis, 1992; Furukubo-Tokunaga et al., 1993; Zeng et al., 1993). In fact, the sequence of the N-terminal arm of the homeodomain that, according to structural determinations, makes direct contacts with DNA is often responsible for these differences (Kissinger et al., 1990; Otting et al., 1990; Wolberger et al., 1991).

Another possibility is that HOM-C proteins act in conjunction with cofactors that modulate their ability to regulate the transcription of downstream genes. Such cofactors could directly affect the DNA binding properties of HOM-C proteins and thereby alter target gene selection. For example, in the yeast Saccharomyces cerevisiae, the homeoprotein MATα2 requires minichromosome maintenance protein MCM1 to bind and repress a specific set of downstream target genes (Keleher et al., 1988). Alternatively, HOM-C cofactors could determine whether a particular target gene is activated or repressed, or they could modulate the degree of activation or repression.

Recently, there has been experimental support for the existence of specificity cofactors for HOM-C proteins. Specifically, five homeodomain amino acids and sequences carboxy-terminal to the homeodomain were shown to be important for distinguishing between the in vivo functions of two closely related Drosophila HOM-C proteins, Ultrabithorax (Ubx) and Antp (Chan and Mann, 1993). Based on the three-dimensional structures of homeodomains bound to DNA (Kissinger et al., 1990; Otting et al., 1990; Wolberger et al., 1991), some of these amino acids are predicted to face away from DNA. Thus, these mapping experiments suggest that the in vivo specificities of HOM-C proteins are in part due to interactions with other proteins.

Further support for the importance of protein–protein interactions is provided by the properties of the *extradenticle* (*exd*) gene which, by genetic criteria, modulates the in vivo functions of HOM-C proteins (Peifer and Wieschaus, 1990). In particular, mutations in *exd* cause homeotic transformations in thoracic and abdominal segments without altering the expression patterns of the HOM-C genes. Therefore, HOM-C proteins, including Antp and Ubx, are correctly expressed in *exd*⁻ embryos but specify incorrect segmental patterns. *exd* encodes an unusual homeodomain protein that is highly related to the mammalian homeobox-containing proto-oncogene, *pbx1* (Flegel et al., 1993; Rauskolb et al., 1993). The expression pattern of *exd* predicts that exd protein will be present at the same time and place as many HOM-C proteins, including Ubx and Antp (Rauskolb et al., 1993). Thus, the genetic and molecular analysis of *exd* suggests that it could encode a cofactor that modulates the in vivo functions of HOM-C proteins.

To characterize how exd modulates the functions of

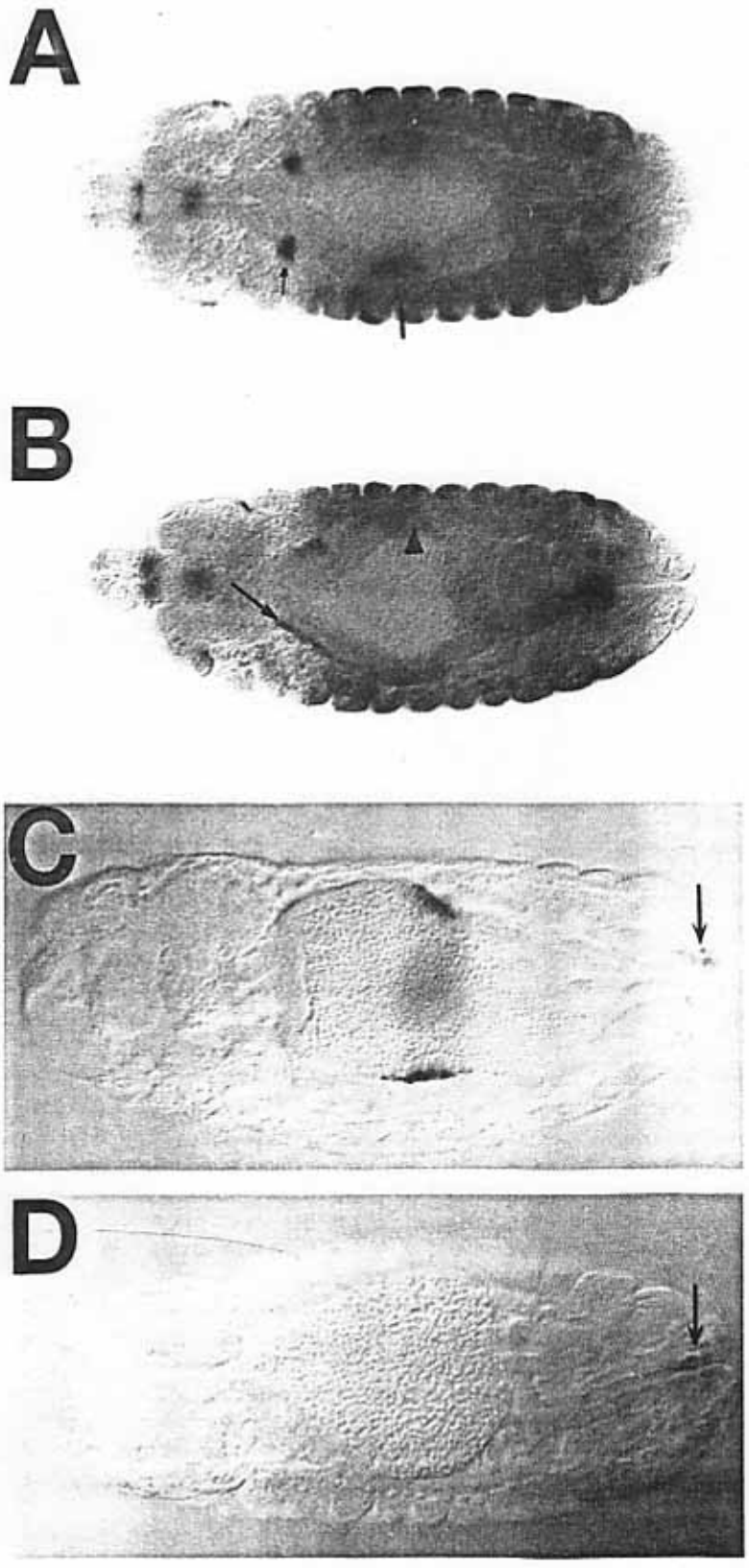

Figure 1. *exd* Is Required for *dpp* Expression and *dpp303* Activity In Vivo

(A and B) Wild-type (A) and *exd*⁻ (B) embryos were doubly stained for dpp (blue/black) and Ubx (brown) proteins. In wild-type embryos, dpp is expressed very strongly in PS7 of the visceral mesoderm (thick arrow), more weakly in the primordia of the gastric caeca (thin arrow), and in several places in the head and the hindgut. Ubx is also expressed in PS7 of the visceral mesoderm, but it is not visible owing to strong dpp expression. In *exd*⁻ embryos, dpp expression in PS7 is very weak and the gastric caeca expression is nearly eliminated. Weak ectopic expression anterior to PS7 in the visceral mesoderm is visible (thin arrow), and the hindgut and head staining appear to be unaffected. In *exd*⁻ embryos, Ubx expression is normal in ps 7 of the visceral mesoderm (arrowhead).

(C and D) Wild-type (C) or *exd*⁻ (D) *dpp303–lacZ* embryos stained for lacZ expression. As with *dpp* expression, *exd* is required for *dpp303* activity. The thin arrows in (C) and (D) point to weak, line-specific staining that is used as an internal control for staining levels because it is unaffected in *exd* mutant embryos. The embryos in (A) and (B) and (C) and (D), respectively, were fixed and stained in parallel; thus, the levels of staining are directly comparable.

HOM-C proteins, we studied a 303 bp enhancer element (*dpp303*) from the Drosophila *decapentaplegic* gene (*dpp*) (Capovilla et al., 1994). *dpp* encodes a member of the transforming growth factor β family, and its expression in parasegment 7 (PS7) of the visceral mesoderm is necessary for a morphogenetic constriction of the embryonic midgut (Padgett et al., 1987; Immergluck et al., 1990; Panganiban et al., 1990; Reuter et al., 1990). Direct binding of Ubx to the *dpp303* enhancer is required for its activation in PS7 of the visceral mesoderm (Capovilla et al., 1994). In contrast, Antp, which is expressed anterior to PS7, does not activate this enhancer. In the experiments described here, exd is shown to bind cooperatively with Ubx, but not with Antp, to binding sites within the *dpp303* enhancer. As exd and Ubx are both required for *dpp* expression in this tissue, we suggest that this cooperative interaction is important in vivo. Thus, the developmental specificity of HOM-C proteins may be conferred at least in part by cofactors such as exd that selectively modulate their DNA binding specificities.

Results

exd Is Required for *dpp* Expression and *dpp303* Activity In Vivo

Wild-type expression of *dpp* in PS7 of the visceral mesoderm requires the coincident expression of *Ubx* (Padgett et al., 1987; Immergluck et al., 1990; Panganiban et al., 1990; Reuter et al., 1990). This aspect of *dpp* expression, including the dependency on *Ubx*, can be mimicked by using a 303 bp enhancer element (*dpp303*) from the *dpp* gene to drive the expression of a reporter gene (Capovilla et al., 1994). If *exd* also plays a role in *dpp* expression in this tissue, then embryos that lack exd function should have altered *dpp* expression. As *exd* is expressed both maternally and zygotically (Rauskolb et al., 1993), embryos devoid of all exd function were examined. In the complete absence of *exd*, the expression of *dpp* (Figures 1A and 1B) and of the *dpp303–lacZ* reporter gene (Figures 1C and 1D) in PS7 of the visceral mesoderm was greatly reduced. In addition, *dpp* expression in the gastric caeca primordia was nearly eliminated, and weak ectopic expression of *dpp* anterior to PS7 in the visceral mesoderm was observed (Figure 1B). In contrast, Ubx expression was normal in *exd*$^-$ embryos, demonstrating that the lower levels of dpp in PS7 were not due to the lack of Ubx (Figure 1B). Thus, *Ubx* and *exd* act in parallel to activate *dpp* in PS7 of the visceral mesoderm. In addition, *exd* appears to be required to repress *dpp* expression in the visceral mesoderm anterior to PS7. Similar observations to these, including the effects on the *dpp303* enhancer, have been made independently by Rauskolb and Wieschaus (1994).

Exd-Binding Sites Are Close to Ubx-Binding Sites

For most of the experiments described here, the source of exd protein was a bacterially expressed fusion between a His-tag sequence and a fragment of exd containing its homeodomain (see Experimental Procedures for details) (Smith et al., 1988). Unless otherwise stated, all HOM-C proteins used in this study were also fusions with the His-tag sequence and included their homeodomains and all carboxy-terminal sequences. All fusion proteins were purified using Ni$^+$ affinity chromatography after their overexpression in Escherichia coli (Smith et al., 1988).

Initially, the *dpp303* DNA fragment was scanned for exd-binding sites using the electrophoretic mobility shift assay (EMSA) with purified exd protein. At least three regions of *dpp303* were observed to have specific binding sites (data not shown). We focused our attention on an 80 bp fragment located at the 5′ end of *dpp303* in which Ubx- and exd-binding sites are clustered (see below). This fragment (*dpp80*) contains two Ubx-binding sites, referred to as sites 4a and 4b (Capovilla et al., 1994). *dpp80* is likely to have weak enhancer activity in vivo because a slightly larger fragment, containing the same and no additional high affinity exd- and Ubx-binding sites, can direct Ubx- and exd-dependent expression in PS7 of the visceral mesoderm (data not shown).

DNAaseI protection was used to map the exd- and Ubx-binding sites in *dpp80* (data not shown; Capovilla et al., 1994; summarized in Figure 2A). Exd protects two regions that are close to and partially overlap the Ubx-protected regions (Figure 2A). Within the regions protected by exd are the sequences 5′-ATCGAAATG-3′ and 5′-ATAAAACAA-3′, which are related to the optimized binding site identified for one of the human exd homologs, pbx1 (5′-ATCAATCAA-3′) (Van Dijk et al., 1993). These exd-binding sites were confirmed by demonstrating that mutations in these sequences completely eliminated specific exd binding to *dpp80* (see below).

To confirm that the DNAaseI protection was due to a pbx-like binding activity, exd binding to *dpp80* was measured in the presence of specific and nonspecific competitor DNAs (Figure 2B). Using EMSA to analyze the products, a single, slower mobility complex was observed with 0.2 μg of exd (Figure 2B, lane 3), and an additional complex was observed with 2.0 μg of exd (Figure 2B, lane 4). These data are consistent with *dpp80* containing two exd-binding sites. The formation of these complexes was largely prevented by adding increasing amounts of an oligonucleotide containing the pbx consensus-binding site, 5′-ATCAATCAA-3′ (Van Dijk et al., 1993) (Figure 2B). In contrast, increasing amounts of the nonspecific competitor poly(dI)–(dC) (up to a 500-fold excess; Figure 2B, lane 10) did not reduce the amount of complex formation. Thus, exd binding to *dpp80* is specific for the pbx-like binding sites present on this DNA fragment.

Exd and Ubx Bind Cooperatively to *dpp80*

The arrangement of Ubx- and exd-binding sites in *dpp80* suggested that these two proteins may interact upon binding to this fragment. This was tested using EMSA to analyze the complexes that form in the presence of either protein alone or in combination (Figure 3). In all cases, when both exd and Ubx were present in a binding reaction, the total amount of bound *dpp80* was significantly greater than the sum of the amounts bound by each protein alone.

Ubx binding to *dpp80* was measured in the absence and presence of two different amounts of exd (Figures 3A–3C). By itself, increasing amounts of Ubx generated

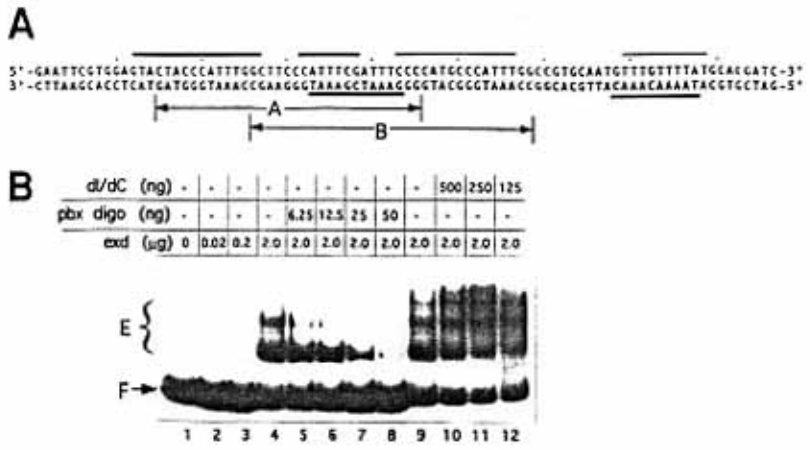

Figure 2. *dpp80* Contains Exd–Pbx-Binding Sites

(A) The sequence of *dpp80*. The binding sites identified by DNAaseI protection for Ubx (overlines) and exd (underlines) are indicated. Thinner lines represent weaker binding sites. The A and B regions delineate the oligonucleotides *dpp80A* and *dpp80B*, respectively (see Figure 3).

(B) Exd binding to *dpp80* is specifically competed by an oligonucleotide containing a pbx-binding site (pbx oligo). In addition to the reagents indicated, all reactions contained 0.5–1.0 ng of [^{32}P]*dpp80* and 125 ng of poly(dI)–(dC).

Abbreviations: F, free probe; E, exd–*dpp80* complexes; and (dI)/(dC), poly(dI)–(dC).

first one, then two Ubx–*dpp80* complexes (U complexes; Figure 3A). When 1.5 μg of exd was included in the reaction, additional slower mobility complexes were observed (U–E complexes; Figure 3B). In addition, the slower of the two U complexes was observed at much lower Ubx concentrations in the presence of exd than in its absence (compare Figure 3B, lane 3 with Figure 3A, lane 6). Quantitation of these data demonstrates that the total amount

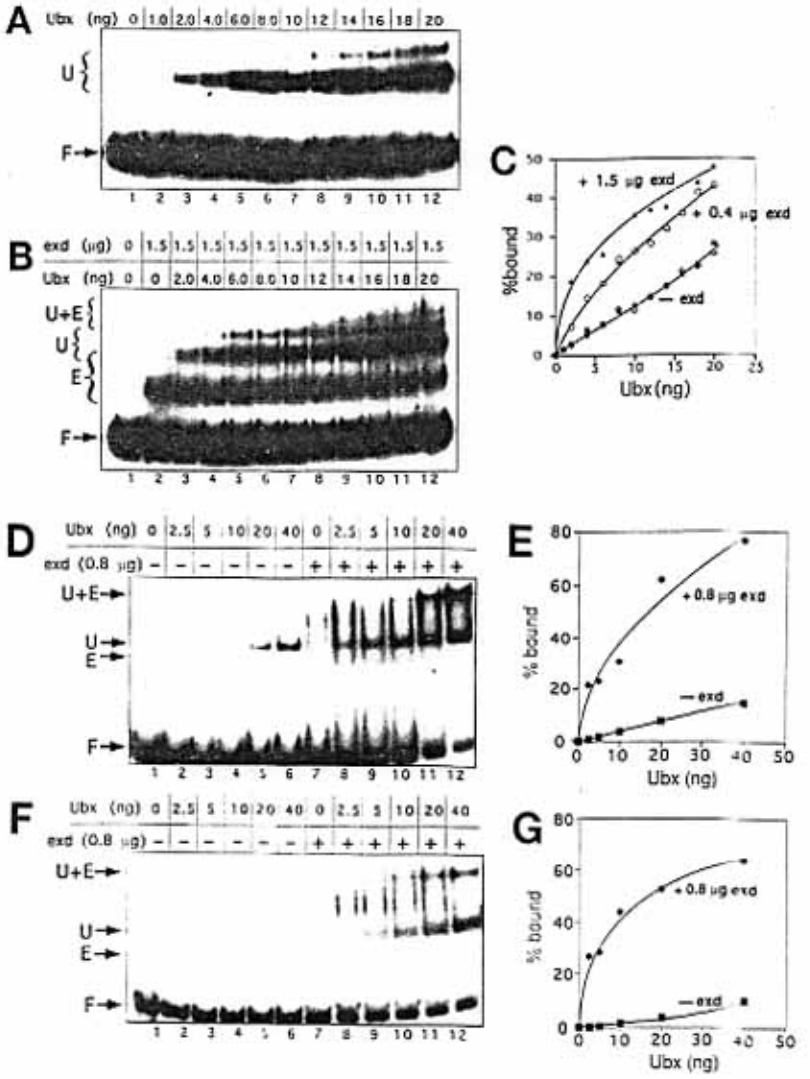

Figure 3. Cooperative Binding of Ubx and Exd to *dpp80*

(A–C) Cooperative binding to *dpp80*. Increasing amounts of Ubx in the absence (A) and presence (B) of 1.5 μg of exd were incubated with [^{32}P]*dpp80*, and EMSA was used to display the products. (C) Quantitation of the data in (A) and (B). In addition, a second independent set of data from a Ubx titration in the absence of exd (diamonds) and the results of a similar Ubx titration in the presence of 400 ng of exd (circles) are presented. The total percentage of bound *dpp80* is plotted as a function of Ubx concentration. The data points representing the percentage bound owing to increasing amounts of Ubx in the presence of either 400 ng of exd (circles) or 1.5 μg of exd (triangles) have all been subtracted by the percentage bound by exd alone (approximately 5% and 30%, respectively). Thus, the difference between these curves and the without exd (–exd) curve (diamonds or squares) represents the amount of synergistic binding resulting from both proteins being present in the reaction.

Abbreviations: F, free probe; E, exd–*dpp80* complexes; U, Ubx–*dpp80* complexes; and U–E, or U+E, Ubx- and exd-dependent complexes.

(D–G) Cooperative binding to *dpp80* subfragments. [^{32}P]*dpp80A* (D) and *dpp80B* (F) were incubated with increasing amounts of Ubx in the absence (lanes 1–6) and presence (lanes 7–12) of 800 ng of exd, and EMSA was used to display the products. Abbreviations are as above. (E) is the quantitation of the data in (D), and (G) is the quantitation of the data in (F). The percentage bound in the presence of exd has been subtracted by the amount bound by exd alone. Thus, the difference between the without exd (–exd) curve and the curve showing the addition of 0.8 μg of exd (+ 0.8 μg of exd) represents the amount of synergistic binding resulting from both proteins being present in the reaction.

of bound *dpp80* is synergistically increased in the presence of both proteins (Figure 3C). Using the data from this experiment, apparent binding constants (K_D) were estimated. Under these reaction conditions, the K_D for Ubx binding to *dpp80* in the absence of exd was approximately 1.7×10^{-7} M. In contrast, the addition of either 400 ng or 1.5 μg of exd to the reaction resulted in a K_D for Ubx binding of approximately 6.7×10^{-8} M and 8.9×10^{-9} M, respectively. These reductions in K_Ds correspond to an effective increase in Ubx binding affinity of 2.5- and 18.8-fold, respectively. As this increase in affinity is dependent on exd-binding sites (see below), we interpret these data as the result of cooperative binding between Ubx and exd. Similar conclusions were obtained when the concentration of exd was varied in either the absence or presence of a constant amount of Ubx (data not shown).

Exd and Ubx also bind cooperatively to subfragments of *dpp80* (*dpp80A* and *dpp80B*), suggesting that individual pairs of Ubx- and exd-binding sites are sufficient for this cooperative interaction (see Figure 2A for a description of these fragments). Ubx binding to both *dpp80A* and *dpp80B* was increased approximately 6- to 30-fold by 800 ng of exd (Figures 3E and 3G). At higher concentrations of Ubx, a single slow mobility U–E complex was observed with both subfragments. In addition, the presence of exd in the binding reaction apparently increases the amount of the Ubx–*dpp80* complex (for example, Figure 3D, compare lane 3 with lane 9). This unusual effect may be due to the relative instability of the U–E complexes as measured by EMSA. Alternatively, exd may alter the conformation of *dpp80*, Ubx, or both in such a way as to increase the stability of the U complex. These possibilities are more fully considered in the Discussion.

The Slower Mobility Complexes Contain Ubx

To confirm that the U–E complexes contain Ubx, a monoclonal antibody (mAb) recognizing Ubx carboxy-terminal sequences (the Ubx C-tail) (mAb 5C.2B; Lopez and Hogness, 1991) was added to a set of binding reactions with *dpp80*, and the products were analyzed using EMSA (Figure 4). The addition of mAb 5C.2B resulted in a very slowly migrating complex (the antibody complex) only when Ubx was present (Figure 4, compare lanes 8 and 10). When 1.5 μg of exd was present alone in the reaction, two exd complexes were visible, and no effect due to addition of the antibody was observed (Figure 4, compare lanes 2 and 9). When Ubx and exd were both present in the reaction, a single U–E complex was observed (Figure 4, lane 4). Addition of mAb 5C.2B reduced the amount of this U–E complex and generated the antibody complex (Figure 4, lane 5), confirming the presence of Ubx in this Ubx- and exd-dependent complex.

The amount of the antibody complex is 6-fold greater in the presence of exd than in its absence (Figure 4, compare lanes 5 and 10). This additional exd-dependent supershift of Ubx-containing complexes may be due in part to the cooperative interaction between Ubx and exd on *dpp80*. However, this conclusion is complicated by the fact that mAb 5C.2B can itself stabilize the interaction between Ubx and *dpp80*, even in the absence of exd (see below).

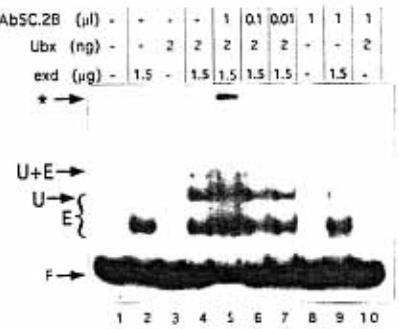

Figure 4. An Exd- and Ubx-Dependent Complex Contains Ubx

Ubx (2 ng) (lanes 3 and 10), 1.5 μg of exd (lanes 2 and 9), or both (lanes 4–7) were incubated with [^{32}P]*dpp80* in the absence (lanes 1–4) or presence (lanes 5–10) of mAb 5C.2B, and EMSA was used to display the products. The amounts of mAb 5C.2B are indicated in microliters of supernatant.

Abbreviations: F, free probe; E, exd complexes; U, Ubx complex; *, the supershifted complex induced by mAb 5C.2B; and U–E, or U+E, Ubx- and exd-dependent complexes.

Exd-Binding Sites Are Required In Vitro and In Vivo

The arrangement of exd- and Ubx-binding sites on *dpp80* suggested that the increase in binding was due to an interaction between Ubx and exd while both proteins are bound to DNA. To test this, a mutant *dpp80* oligonucleotide (*dpp80E2*$^-$) was synthesized containing point mutations within both of the exd-binding sites. As expected, no sequence-specific exd binding to this DNA was observed in EMSA experiments (data not shown). Although Ubx binding to *dpp80E2*$^-$ was approximately 2-fold weaker than was binding to wild-type *dpp80*, both Ubx-binding sites were still recognized (Figure 5A; data not shown). However, over a wide range of concentrations, Ubx binding to *dpp80E2*$^-$ was similar in the absence or presence of 400 ng of exd (Figure 5A). Thus, exd must specifically bind to *dpp80* to increase Ubx binding.

A *dpp303* fragment containing the same mutations as *dpp80E2*$^-$ (*dpp303E2*$^-$) was tested for enhancer activity in vivo. When directly compared with wild-type *dpp303*, *dpp303E2*$^-$ directed much weaker expression of a *lacZ* reporter gene in PS7 of the visceral mesoderm (Figures 5B and 5C). Thus, these exd-binding sites are critical for cooperative interactions with Ubx in vitro and for enhancer activity in vivo.

Exd Stabilizes the DNA-Bound Form of Ubx

One way that exd could increase the affinity of Ubx for *dpp80* is by reducing the dissociation rate of Ubx, thereby stabilizing the DNA-bound form of Ubx. To test this possibility, the dissociation of Ubx and exd from *dpp80* was monitored after complexes were formed by each protein alone or in combination (Figure 6A). Binding reactions were allowed to reach equilibrium and were then challenged with a 500-fold excess of unlabeled *dpp80* for various lengths of time. The concentrations of Ubx and exd used (5 ng and 600 ng, respectively) were limiting so that, at time 0, predominantly single complexes are formed by either protein alone (Figure 6A, lanes 1 and 13). At these concentrations, the products present at time 0 when both

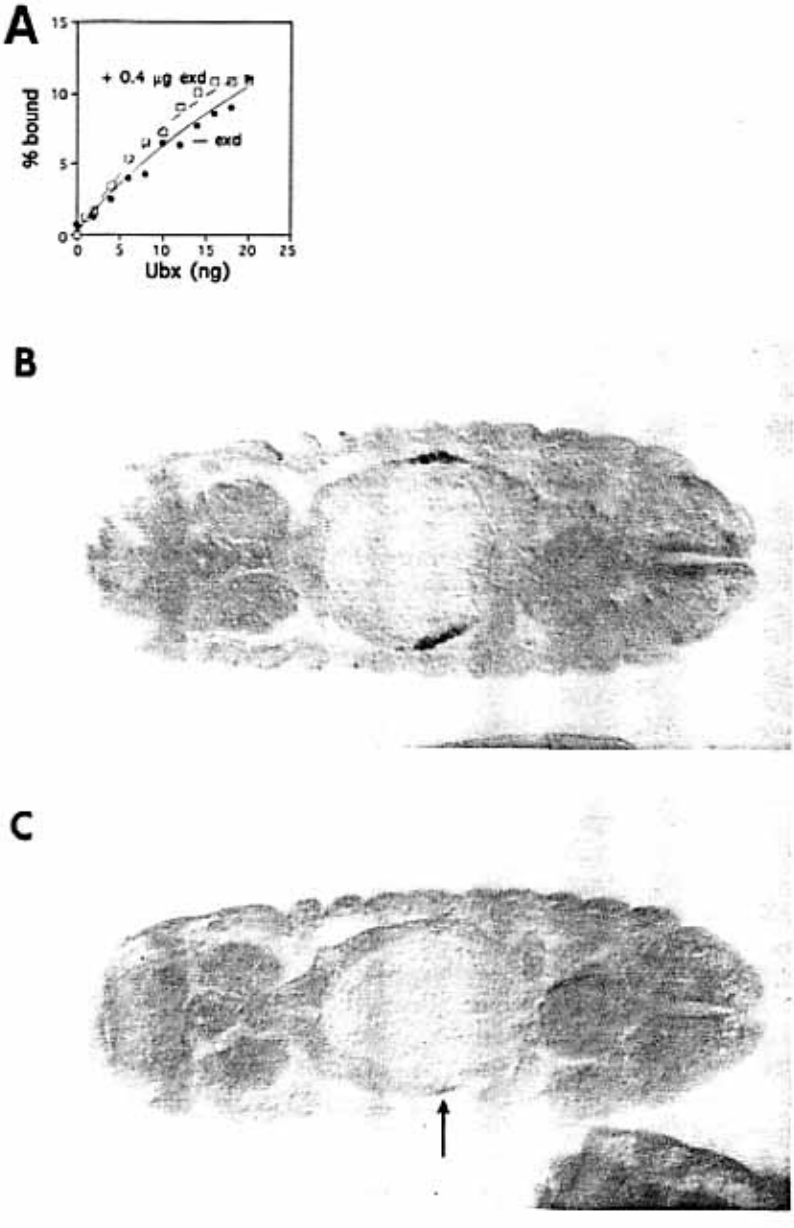

Figure 5. Exd-Binding Sites Are Important In Vitro and In Vivo

(A) Increasing amounts of Ubx in the absence (circles) and presence (squares) of 400 ng of exd were incubated with *[^{32}P]dpp80E2$^-$* DNA (a *dpp80* oligonucleotide in which both exd-binding sites were destroyed), and the products were analyzed using EMSA. These results have been quantitated and are presented as the total percentage of *dpp80E2$^-$* bound versus the Ubx concentration.

(B and C) *dpp303-lacZ* (B) and *dpp303E2$^-$-lacZ* (C) embryos were stained for *lacZ* expression using anti-β-galactosidase antibody. Expression in PS7 of the visceral mesoderm is strong in (B) and barely detectable in (C, arrow).

proteins are present include at least one U–E complex (Figure 6A, lane 7). Furthermore, as described above (see Figure 3), when both exd and Ubx are present, the amount of U complex formed is greater than that generated by Ubx alone (Figure 6A, compare lanes 1 and 7).

By themselves Ubx and exd have dramatically different dissociation rates. After 1 min in the presence of the unlabeled competitor, greater than 98% of the complexes formed in the presence of Ubx alone have dissociated (Figure 6A, lane 2). In contrast, 100% of the complexes formed in the presence of exd alone remain stable for at least 30 min (Figure 6, lane 18). When both Ubx and exd are present, 10% of the U–E complex is still present after 30 min (Figure 6, lane 12). Moreover, a significant fraction of the U complex formed in the presence of exd is also stable (approximately 11% remains after 30 min; Figure 6, lane 12). These results indicate that the rate of dissociation of Ubx from *dpp80* is reduced in the presence of exd.

Confirmation that these stable, slower mobility complexes observed in the presence of Ubx and exd contain Ubx was obtained by monitoring the dissociation of these complexes in the presence of mAb 5C.2B (Figure 6B). As expected, both the U and U–E complexes were efficiently supershifted in the presence of the antibody, whereas the complex containing only exd was not affected (compare Figure 6A, lanes 7–12 with Figure 6B, lanes 1–6). However, to our surprise, addition of mAb 5C.2B to a binding reaction containing Ubx alone also stabilized the interaction between Ubx and *dpp80* (Figure 6B, lanes 7–10). The resulting antibody complex, which probably contains *dpp80*, Ubx, and mAb 5C.2B, did not dissociate during the time course of the experiment. As mAb 5C.2B recognizes an epitope within the C-tail of Ubx, this result suggests that the stabilization of Ubx binding to *dpp80* by this antibody and possibly by exd as well is due to an interaction with the Ubx C-tail.

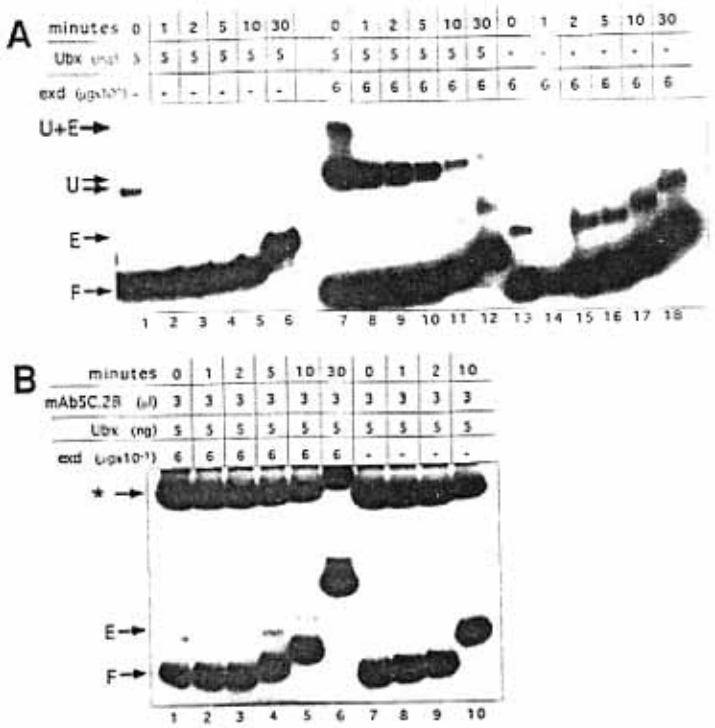

Figure 6. Exd Decreases the Rate That Ubx Dissociates from *dpp80*

(A) Ubx (5 ng, lanes 1–6), 600 ng of exd (lanes 13–18), or both (lanes 7–12) were incubated with [^{32}P]*dpp80*. After 1 hr, a 500-fold excess of unlabeled *dpp80* was added for increasing amounts of time as indicated.

Abbreviations: F, free probe; E, exd–*dpp80* complex; U, Ubx–*dpp80* complex; and U–E, or U+E, Ubx- and exd-dependent complexes.

(B) Ubx (5 ng, lanes 1–10), 600 ng of exd (lanes 1–6), and 3 μl of mAb 5C.2B supernatant (lanes 1–10) were incubated with [^{32}P]*dpp80*. After 1 hr, a 500-fold excess of unlabeled *dpp80* was added for increasing amounts of time as indicated. Because these samples were loaded during electrophoresis, the complexes present at the later time points have migrated less far than those present at the earlier time points.

Abbreviations: F, free probe; E, exd–*dpp80* complex; and *, mAb 5C.2B-induced supershifted complex.

Exd Does Not Cooperatively Bind with Antp on *dpp80*

The *dpp303* enhancer is active in PS7 of the visceral mesoderm but inactive in more anterior and posterior parasegments of this tissue (Capovilla et al., 1994). Antp, therefore, which is present in the visceral mesoderm anterior to PS7 (Tremml and Bienz, 1989), does not activate *dpp303*. One possible explanation for this differential response of *dpp303* to Ubx and Antp is that exd cooperatively binds with Ubx but not with Antp. This was tested for *dpp80* by measuring Antp binding to this fragment in the presence and absence of exd (Figure 7).

With increasing amounts of Antp, first one and then a second slower mobility complex was observed, demonstrating that Antp binds to *dpp80* (Figure 7A). Although the amount of Antp required is greater than the amount of Ubx required, the binding of Antp to *dpp80* is qualitatively similar to that seen with increasing amounts of Ubx (see Figure 3A). However, only a weak enhancement of Antp binding by exd was observed (Figures 7B and 7C). At low concentrations of Antp, the amount of *dpp80* bound is similar in the presence or absence of 400 ng of exd. At higher concentrations of Antp, a small increase (less than 1.5-fold) was observed in the presence of exd. A similarly weak enhancement of Antp binding to *dpp80* was also observed in the presence of 1.5 μg of exd (data not shown). Exd–*dpp80* complexes were formed in the presence of Antp, demonstrating that Antp does not prevent exd binding. These results suggest that, with respect to binding to *dpp80*, exd specifically interacts with Ubx, but not with Antp.

In addition to these in vitro DNA binding experiments, we tested if a specific interaction between Ubx and exd could be observed in the absence of DNA. To this end, the yeast two-hybrid system was used (Chien et al., 1991). In these experiments, the GAL4 DNA-binding domain was fused to the Ubx homeodomain and C-tail (GDB–Ubx) or an equivalent fragment from Antp (GDB–Antp). The GAL4 activation domain was fused to almost the entire exd open reading frame (GAD–exd; see Experimental Procedures). An interaction between exd and either Ubx or Antp was assessed by measuring the activation of a UAS_{GAL4}–*lacZ* reporter gene. Individually, GAD–exd and GDB–Antp did not activate the UAS_{GAL4}–*lacZ* gene (Table I). GDB–Ubx weakly activated UAS_{GAL4}–*lacZ* when present by itself. However, when both GDB–Ubx and GAD–exd were present together, a 3- to 4-fold increase in activation above that produced by GDB–Ubx alone was observed. In contrast, combining GDB–Antp plus GAD–exd did not activate the UAS_{GAL4}–*lacZ* gene (Table I). These data support the conclusions from the in vitro DNA binding experiments that exd can specifically interact with the Ubx homeodomain plus C-tail, but not with the equivalent fragment of Antp. Furthermore, the yeast interaction experiments suggest that exd can interact with Ubx in the absence of specific DNA-binding sites.

The Importance of Ubx Homeodomain Residues Thr-23, His-25, and Leu-57

Using Ubx–Antp chimeric proteins, homeodomain residues Thr-23, His-25, and Leu-57 and the Ubx C-tail were shown to be important to distinguish the in vivo functions of these two homeotic proteins (Chan and Mann, 1993). As these amino acids are in a position to interact with a cofactor, we investigated if these residues were necessary for the interaction between Ubx and exd.

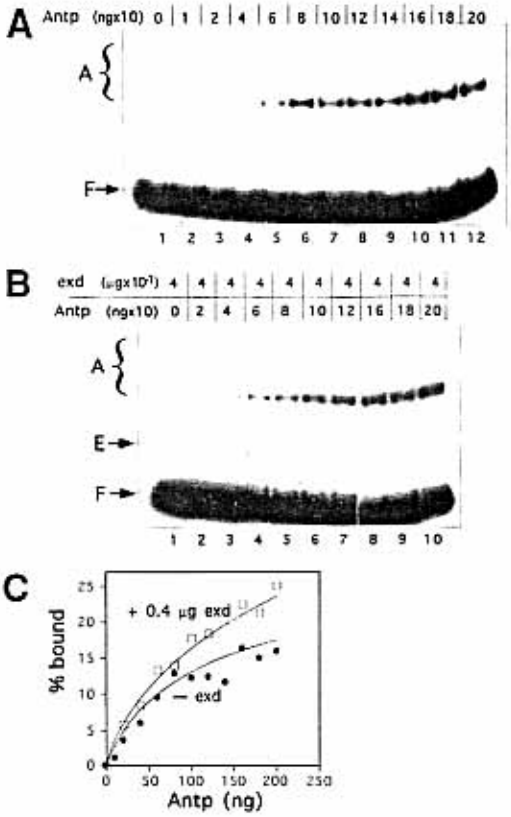

Figure 7. Antp Binding Is Similar in the Absence and Presence of Exd

Increasing amounts of Antp in the absence (A) and presence (B) of 400 ng of exd were incubated with *[³²P]dpp80*, and EMSA was used to display the products. The amounts of Antp are indicated. (C) represents quantitation of the data shown in (A) and (B). The total percentage of bound *dpp80* is plotted as a function of Antp concentration. The data points representing percentage bound owing to increasing amounts of Antp in the presence of 400 ng of exd (squares) have all been subtracted by the percentage bound by 400 ng of exd alone (B, lane 1; approximately 5%). Thus, the difference between these curves represents the amount of synergistic binding due to both proteins being present in the reaction.

Abbreviations: F, free probe; E, exd–*dpp80* complex; and A, Antp–*dpp80* complexes.

The first Ubx mutant studied consists of the identical portion of Ubx used above (homeodomain plus C-tail), except that homeodomain residues 23, 25, and 57 were all changed to alanines. This mutant (GST–Ubx-a3) was fused to the glutathione S-transferase (GST) sequence for purification from E. coli. As a control for these experiments, the wild-type homeodomain and C-tail from Ubx were also fused to GST (GST–Ubx). Both GST–Ubx and GST–Ubx-a3 bound to *dpp80* in the absence of exd (Figure 8A, lanes 3 and 6). However, while the binding of GST–Ubx was stimulated 10-fold by the addition of 800 ng of exd, the binding of GST–Ubx-a3 was stimulated only 1.2-fold (Figure 8A, lanes 5 and 8). These results demonstrate that Ubx homeodomain residues 23, 25, and 57 are important for the in vitro interaction with exd.

In the next experiment, two Ubx–Antp chimeras and a Ubx truncation mutant were studied (Figure 8B). For this experiment, all proteins were fused to the His-tag sequence. The proteins used in this experiment were as follows: the Ubx homeodomain and Ubx C-tail (UU), the Antp homeodomain and Antp C-tail (AA), the Ubx homeodomain and Antp C-tail (UA), the Antp homeodomain and Ubx C-tail (AU), and the Ubx homeodomain with no C-tail (U_{HD}). Binding to *dpp80* in the absence and presence of exd was measured for each of these proteins.

Only UU, containing both the Ubx homeodomain and Ubx C-tail, showed a strong increase in binding in the presence of exd (Figure 8B, lanes 3 and 4). Both Ubx–Antp chimeras and the Ubx homeodomain exhibited no or very weak evidence of an interaction with exd. These results demonstrate that both the Ubx homeodomain and the Ubx C-tail are important for the in vitro interaction with exd.

Table 1. Exd and Ubx Specifically Interact in the Yeast Two Hybrid Assay

DNA-Binding Hybrid	Activation Domain Hybrid	Activity[a]
GDB–Ubx	–	16.1 ± 1.0
–	GAD–exd	2.5 ± 0.4
GDB–Ubx	GAD–exd	54.6 ± 6.7
GDB–Antp	–	1.8 ± 0.6
GDB–Antp	GAD–exd	1.7 ± 0.3
GDB–SNF1[b]	GAD–exd	3.1 ± 0.2

[a] Activity is listed in units of β-galactosidase. These numbers are the averages and standard deviations for six independent measurements.
[b] GDB–SNF1 refers to the GDB fused to the yeast sucrose nonfermenting 1 gene used as a negative control (Durfee et al., 1993).

In Vivo Activation of *dpp* Requires the Ubx Homeodomain and Ubx C-Tail

If the interaction between Ubx and exd is relevant to the activation of *dpp* in vivo, only proteins containing the Ubx homeodomain and Ubx C-tail should be strong activators. This prediction was tested by comparing the extent of *dpp* activation induced by the ubiquitous expression of Ubx and of Ubx–Antp chimeric proteins. Ubiquitous expression of wild-type Ubx (via the *hsp70* promoter) strongly activates dpp expression throughout the anterior half of the visceral mesoderm (Figure 8C) (Reuter et al., 1990). In contrast, ubiquitous expression of UAU protein, in which the Ubx homeodomain is replaced by the Antp homeodomain, did not result in the ectopic activation of *dpp* (Figure 8D). Furthermore, ubiquitous expression of UU_{stop} protein, which is truncated immediately following the Ubx homeodomain and thus contains no C-tail, resulted in very weak ectopic *dpp* activation (Figure 8E). Thus, the Ubx homeodomain and Ubx C-tail are both important for activating *dpp* expression in the visceral mesoderm. As these portions of Ubx are also critical for the in vitro interaction with exd, these results suggest that a direct interaction between Ubx and exd mediated by the Ubx homeodomain and C-tail is important for *dpp* activation in vivo.

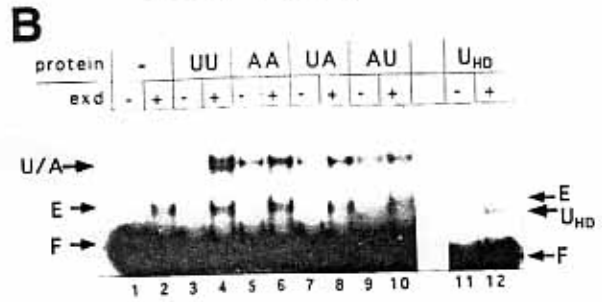

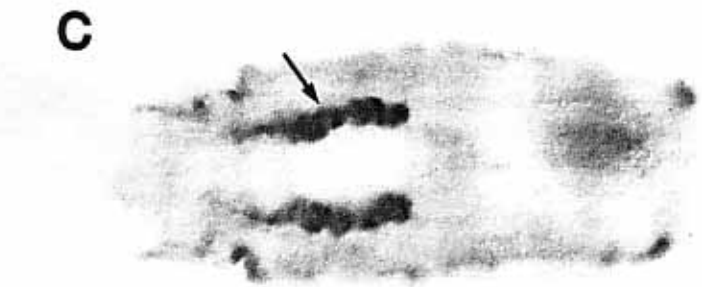

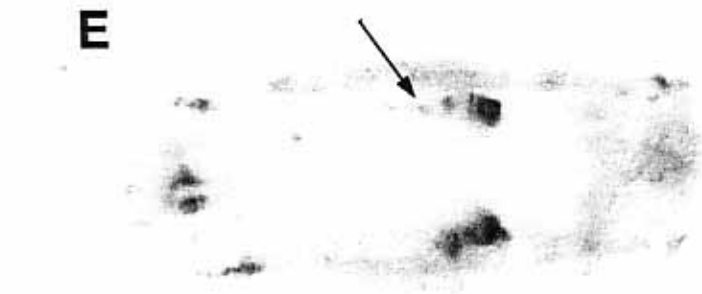

Figure 8. Optimal Interaction with Exd Requires the Ubx Homeodomain and Ubx C-Tail

(A) Changing three Ubx homeodomain residues, Thr-23, His-25, and Leu-57, to alanines blocks the interaction with exd. Exd (400 ng, lanes 1, 4, and 7 or 800 ng, lanes 2, 5, and 8) was incubated with no Ubx (lanes 1 and 2), 2 ng of GST–Ubx (lanes 3–5), or 4 ng of GST–Ubx-a3 (lanes 6–8) in the presence of [^{32}P]*dpp80*, and the products were analyzed using EMSA. The amount of GST–Ubx-a3 was greater than the amount of GST–Ubx, resulting in more U complex formed in the absence of exd (lanes 3 and 6).

Abbreviations: F, free probe; E, exd–*dpp80* complexes; and U, Ubx–*dpp80* or Ubx-a3–*dpp80* complexes.

(B) Both the Ubx homeodomain and Ubx C-tail are required for optimal cooperative binding with exd. HOM-C proteins were incubated in the presence (lanes 2, 4, 6, 8, 10, and 12) or absence (lanes 1, 3, 5, 7, 9, and 11) of 400 ng of exd and [^{32}P]*dpp80*, and the products were analyzed using EMSA. Lanes 11 and 12 are from a different gel than lanes 1–10 to better resolve the Ubx homeodomain complex from the free probe.

Abbreviations: UU, Ubx homeodomain plus Ubx C-tail; AA, Antp homeodomain plus Antp C-tail; UA, Ubx homeodomain plus Antp C-tail; AU, Antp homeodomain plus Ubx C-tail; U_{HD}, Ubx homeodomain with no C-tail; F, free probe; E, exd–*dpp80* complex; U_{HD}, Ubx homeodomain–*dpp80* complex; and U/A, complexes generated by UU, AA, UA, or AU.

(C–E) Ectopic *dpp* activation by Ubx requires the Ubx homeodomain and Ubx C-tail. Shown here are *HS:Ubx* (C), *HS:UAU* (D), and *HS:* UU_{Antp} (E). Arrows point to ectopic *dpp* expression induced strongly by Ubx (C) and very weakly by UU_{Antp} (E).

Discussion

The Functional Significance of the Ubx-Exd Interaction

Despite very different in vivo functions, HOM-C proteins have overlapping and not very specific in vitro DNA binding specificities (Hayashi and Scott, 1990). The experiments presented here describe one possible mechanism that can account for this apparent paradox. Specifically, we describe a cooperative interaction between Ubx and exd upon binding to a cluster of binding sites within a PS7 visceral mesoderm enhancer from the *dpp* gene. Exd increases the apparent affinity of Ubx for these binding sites by 3- to 30-fold. This cooperative effect is strongest at low Ubx protein concentrations and requires exd-binding sites. In contrast, Antp and exd interact very weakly in this assay (less than 1.5-fold increase in binding is observed) and do so only at high Antp protein concentrations. Therefore, for this enhancer element, exd can differentially modulate the DNA binding properties of these two HOM-C proteins. Based on these results, we suggest that at least one exd function is to help HOM-C proteins select the correct sets of target genes in vivo.

These results are consistent with the fact that both Ubx and exd are required for the activity of this enhancer and for *dpp* expression in vivo (Figure 1; Rauskolb and Wieschaus, 1994). In addition, they are also consistent with the fact that the *dpp303* enhancer is not activated by Antp (Figure 1; Capovilla et al., 1994). However, as there are additional exd- and Ubx-binding sites present in this enhancer (S.-K. C. and R. S. M., unpublished data; Capovilla et al., 1994), the cooperative binding described here may only represent a part of the exd-mediated functions that are necessary for the complete regulation of this enhancer in vivo.

In addition to coregulating *dpp* expression, exd is also required for Ubx to generate a PS6 identity (Peifer and Wieschaus, 1990). This identity, primarily defined by an embryonic cuticle morphology, probably requires the coordinate regulation of many *Ubx* target genes. Therefore, we suggest that similar cooperative interactions between Ubx and exd exist at the regulatory elements of many of these genes as well. Furthermore, it is likely that exd interacts with other HOM-C proteins in addition to Ubx because mutations in exd alter the identities of many segments in Drosophila. In principle, this proposed function for exd may determine whether a particular target gene is bound at all by a HOM-C protein or, alternatively, it may affect the overall amount of binding. Thus, depending on the particular target gene, an interaction with exd could lead to various degrees of HOM-C-binding site occupancy and, therefore, various degrees of repression or activation. Presumably, additional factors recognize the exd–HOM-C–DNA complex and dictate the ultimate regulation of the target gene.

It is also likely that exd has regulatory functions that are independent of the HOM-C genes. One such function may be to repress *dpp* in the anterior visceral mesoderm (Figure 1; Rauskolb and Wieschaus, 1994). Moreover, in the absence of all five HOM-C proteins required for thoracic and abdominal segment identities in Drosophila, mutations in *exd* still alter segment identities (R. S. M., unpublished data). This view is analogous to transcriptional regulation in the yeast S. cerevisiae, where the protein MCM1, which alters the DNA binding properties of the homeoprotein MATα2, also has its own MATα2-independent functions (Keleher et al., 1988).

How Do Exd and Ubx Interact upon Binding to *dpp80*?

For most of the in vitro DNA binding experiments described here, the portion of exd used includes only its homeodomain and several residues N-terminal to the homeodomain. Therefore, the homeodomain of exd is probably sufficient for the observed interaction with Ubx. Furthermore, because Ubx, but not Antp, interacts with exd on this DNA, amino acids in Ubx that are necessary for this interaction were identified (Figures 7 and 8). These experiments showed that three homeodomain residues and the Ubx C-tail, elements that are important for Ubx-specific functions in vivo (Chan and Mann, 1993), are required for this interaction.

These results suggest a direct protein–protein interaction between Ubx and exd for several reasons. First, in a three-dimensional model of the homeodomain bound to DNA, homeodomain residues 23, 25, and 57 and the C-tail are all potentially close to each other in the folded protein and face away from the DNA (Chan and Mann, 1993). These amino acids are therefore in a position to interact with a cofactor such as exd. Second, differences in these amino acids do not alter the in vitro DNA binding specificity of HOM-C proteins (Treisman et al., 1992; S.-K. C. and R. S. M., unpublished data). Third, the yeast two-hybrid experiments suggest that exd and Ubx proteins can directly and specifically interact with each other. Finally, there are at least three other cases where sequences immediately adjacent to a homeodomain have been implicated in mediating protein–protein interactions (Johnson, 1993; Vershon and Johnson, 1993; Xue et al., 1993). Given these results, it seems likely that the portion of the homeodomain that includes amino acids 23, 25, and 57, together with C-terminal sequences, defines a protein interaction surface used by many homeoproteins to contact cofactors.

The stabilizing effect of mAb 5C.2B on Ubx binding to *dpp80* provides further evidence for the importance of the Ubx C-tail (Figure 6). One explanation of this effect is that the C-tail, which may have a disordered structure on its own, destabilizes the binding of Ubx to DNA. Indeed, structural studies on the Antp and MATα2 homeoproteins demonstrate that their C-tails are unstructured (Billeter et al., 1990; Wolberger et al., 1991). The binding of mAb 5C.2B may impose a structure on the C-tail, thus stabilizing the complex. Exd may act similarly to stabilize Ubx binding by also interacting with the C-tail. However, one important difference between these two effects is that exd requires a DNA-binding site to effectively stabilize the complex, whereas the mAb has little or no affinity for DNA (Figure 4). It is possible that the exd–C-tail interaction is weaker than the mAb–C-tail interaction and thus requires additional contacts with DNA to stabilize the ternary complex.

One unusual feature of the cooperative interactions described here is that some of the exd-induced stabilization of Ubx binding can occur without exd being present in the final complex (Figures 3 and 6). Similar effects to these have been observed with the binding of paired-like homeobox protein Phox1 and serum response factor (Grueneberg et al., 1992). One intriguing explanation is that exd may alter the conformation of either the DNA or of Ubx such that the U complex generated in the presence of exd is different from that generated in its absence. According to this view, exd may have a chaperone-like function that induces a more stable interaction between Ubx and DNA. In this way, exd need not be part of the final complex to stimulate Ubx binding. Alternatively, U–E complexes may predominate in solution, but only a fraction remain intact in the EMSA. A third possibility is that additional proteins not present in these in vitro experiments function in vivo to stabilize the exd–Ubx–DNA complex. Although additional experiments are required to understand this phenomenon, the nonlinear rates of dissociation of the U–E and U complexes suggest that multiple conformation states exist for both of these complexes (Figure 6; data not shown).

Implications for Phenotypic Suppression

When two homeotic genes are expressed in the same segment, the resulting segment identity is usually governed by only 1 of the 2 (Gonzalez-Reyes and Morata, 1990; Gonzalez-Reyes et al., 1990; Mann and Hogness, 1990). This effect, termed phenotypic suppression, also applies to the regulation of the *dpp* gene in the visceral mesoderm. Ubiquitous expression of Ubx from a heat shock promoter causes the activation of *dpp* anterior to its normal domain of expression in PS7 (Figure 8; Reuter et al., 1990). In contrast, ubiquitous Ubx expression does not activate *dpp* posterior to PS7 because Ubx cannot override repression by the HOM-C genes *abdominal A* and *Abdominal B*. One explanation for this is that HOM-C proteins compete for DNA-binding sites (Gibson and Gehring, 1988; Gonzalez-Reyes and Morata, 1990). The results presented here suggest two additional possibilities. First, HOM-C proteins may compete for an interaction with exd. Second, the binding of some HOM-C proteins may block exd binding, which would, in the case of *dpp80*, effectively discriminate against Ubx binding.

Implications for the Function of the *pbx* Genes

Three human *exd* homologs, *pbx1*, *pbx2*, and *pbx3*, each encode proteins that share greater than 70% amino acid identity to exd (Monica et al., 1991; Flegel et al., 1993; Rauskolb et al., 1993). This remarkable conservation, which extends over 270 amino acids, suggests that the pbx proteins have similar functions to exd. Thus, as suggested here for exd, pbx proteins may be an important component of an in vivo HOM-C-binding site. Interactions with pbx proteins may stabilize HOM-C–DNA interactions and, depending on the particular binding site, these interactions may be specific for individual HOM-C proteins. The existence of three *pbx* genes in humans suggests the possibility that each one specifically interacts with a different subset of HOM-C proteins. As nearly 25% of pediatric pre–B acute lymphoblastic leukemias are caused by fusions between pbx1 and the helix-loop-helix protein E2A (Kamps et al., 1990; Nourse et al., 1990), it seems reasonable to suggest that these leukemias are caused by HOM-C proteins misregulating the wrong downstream target genes in pre–B cells owing to the inappropriate presence of a pbx1 homeoprotein.

Experimental Procedures

Fly Stocks and Immunohistochemistry

Embryos without maternal and zygotic exd functions were generated by crossing *FRT18 exd y/FM7c* females to heat shock–FLP-containing 18-1F males (Xu and Rubin, 1993). Larvae were shocked for 100 min at 37°C, and *FRT18 exd y/FRT18* females were crossed to *FM7c* males. The frequency of *exd*$^-$ embryos (recognized by their segmentation phenotype; Peifer and Wieschaus, 1990) generated by this cross was monitored by analyzing first instar larval cuticles of collections that paralleled the immunohistochemistry collections. *exd*$^-$ embryos that also contained a *dpp* enhancer fragment driving *lacZ* expression (Figures 1C and 1D) were generated by the following cross: *y w exd*^{P1} *FRT/ovo*^{D} *FRT; hs-FLP38/+* × *y w; dpp303–lacZ/dpp303–lacZ*. Two enhancer fragments were analyzed in vivo: *dpp303* (Capovilla et al., 1994) and *dpp150*, which includes all of *dpp80* and contains the identical set of Ubx- and exd-binding sites as does *dpp80*.

Ubiquitous expression of Ubx, UAU, and UU$_{exd}$ proteins using the *hsp70* promoter has been described (Chan and Mann, 1993). To confirm the ubiquitous expression of these HOM-C proteins, the collections were stained in parallel with anti-Ubx antibody, and homeotic transformations similar to those previously reported (Chan and Mann, 1993) were observed.

The *dpp303* and *dpp303E2–lacZ* stocks used in Figure 5 were generated with the vector CPLZ (Bier et al., 1989). The construction details of these plasmids will be provided upon request. The *dpp303–lacZ* stock used in Figure 1 is described in Capovilla et al. (1994) and differs from *dpp303–CPLZ*.

Immunohistochemistry was performed as described (Chan and Mann, 1993; except for Figures 1C and 1D; see Capovilla et al., 1994). A rabbit anti-dpp polyclonal antibody (Panganiban et al., 1990; provided by M. Hoffmann) was used to detect dpp, the mAb FP3.38 was used to detect Ubx, and a polyclonal mouse anti-β-galactosidase antibody (Cappel) was used to detect *lacZ* expression. The secondary antibodies used were goat anti-mouse, directly conjugated to horseradish peroxidase, and horse anti-rabbit, directly conjugated to alkaline phosphatase (Cappel).

Expression Plasmids

The details of plasmid construction will be provided on request. The Ubx, Antp, UA, AU, and U$_{HD}$ expression plasmids contain the His-tag sequence of pET-His14b (Novagen) fused to homeodomain-containing fragments that begin 3 amino acids before the start of the homeodomain; these peptides include the entire homeodomain and the entire C-tail (when present). The His–exd fusion protein (also in pET-His14b) includes 9 amino acids N-terminal to the exd homeodomain and ends following the entire homeodomain. Expression and purification was as described by the manufacturer. The GST–Ubx, GST–Ubx-a3, and GST–U$_{HD}$ plasmids contained the equivalent fragments of Ubx, Ubx-a3, or UU$_{exd}$ (Chan and Mann, 1993) cloned into the GST–2tK vector (Kaelin et al., 1992). All GST fusion proteins were expressed and purified from E. coli as described (Kaelin et al., 1992). The approximate concentrations of all purified proteins were determined by Bradford assays. Due to the limitations of this assay and to incomplete purification, these assays cannot be used to accurately compare two different protein preparations.

EMSAs

dpp303 (Capovilla et al. 1994) was cloned into Bluescript KS(+) (pdpp303). The *dpp80* fragment was generated by digesting pdpp303 with EcoRI and Sau3A, end-filling with Klenow and [α-^{32}P]dCTP, and gel purifying using standard procedures. The *dpp80E2*$^-$ fragment was synthesized with the following point mutations in the exd-binding sites:

5'-TCCagcggCcgcTTC....TGTggcgccgggGCAC-3', where the small letters represent changes from the wild-type sequence. *dpp80A* and *dpp80B* were chemically synthesized.

EMSA was performed as described with the following modifications (Dessain et al., 1992). For the two experiments using mAb 5C.2B, the gels were 6% acrylamide. In reactions containing both exd and Ubx, exd was added 30 min earlier than was Ubx. In reactions containing mAb 5C.2B, Ubx was preincubated on ice with the antibody for 30 min. The dissociation experiments were performed by incubating standard binding reactions for 60 min, adding 500 ng of unlabeled *dpp80*, and loading a gel while it was running at the various time points. For all EMSA experiments, the gels were dried and quantitated using a direct β emissions scanner (Betagen). The experiments presented in Figures 3A and 3B and Figures 7A and 7B, respectively, were done in parallel with the same probe and are therefore directly comparable.

The Yeast Two-Hybrid System

The GAL4 DNA-binding fusion vector, pAS1–GAL4, and Y153 yeast strain were gifts from S. Elledge (Durfee et al., 1993). pGDB–Ubx consists of the 430 bp homeodomain-containing RsaI fragment cloned in frame into a blunted BamHI site of pAS1–GAL4. pGDB–Antp consists of the 445 bp RsaI fragment from pUAA (Chan and Mann, 1993) cloned in frame into a blunted BamHI site of pAS1–GAL4. The pGAD activation domain vector was a gift from J. Luban (Luban et al., 1993). pGAD–exd contains a 1283 FspI to SnaBI fragment from KS(exd) provided by C. Rauskolb (Rauskolb et al., 1993) cloned in frame into a blunted NotI site of pGAD.

Quantitation of β-galactosidase activities were done as described (Durfee et al., 1993). Values were averaged from at least six independent transformants.

Acknowledgments

We are grateful to Cordelia Rauskolb and Eric Wieschaus for sending the *exd* cDNA and for sharing their results before publication. We also thank Javier Lopez and Michael Hoffmann for antibodies, Cornelius Murre for sharing results prior to publication, the Indiana Stock Center for fly stocks, and Steve Elledge and Jeremy Luban for yeast two-hybrid reagents. We are also indebted to Jin Jiang and Robin Wharton for advice with the EMSA and DNAaseI protection assays and to Richard Axel, Paul Feinstein, Boyana Konforti, Anna Marie Pyle, and Gary Struhl for excellent suggestions regarding these experiments and critical comments on this manuscript. This work was supported by the National Institutes of Health, Searle Foundation, and March of Dimes grants awarded to R. S. M. and by National Science Foundation and March of Dimes grants awarded to J. B. We also gratefully acknowledge the International Human Frontier Science Program for supporting the continuing collaboration between the laboratories of R. S. M. and J. B.

Received March 14, 1994; revised July 8, 1994.

References

Andrew, D. J., and Scott, M. P. (1992). Downstream of the homeotic genes. New Biol. *4*, 5–15.

Bier, E., Vaessin, H., Shepherd, S., Lee, K., McCall, K., Barbel, S., Ackerman, L., Carretto, R., Uemura, T., Grell, E., Jan, L. Y., and Jan, Y. N. (1989). Searching for pattern and mutation in the *Drosophila* genome with a P–*lacZ* vector. Genes Dev. *3*, 1273–1287.

Billeter, M., Qian, Y., Otting, G., Muller, M., Gehring, W. J., and Wuthrich, K. (1990). Determination of the three-dimensional structure of the Antennapedia homeodomain from *Drosophila* in solution by 1H nuclear magnetic resonance spectroscopy. J. Mol. Biol. *214*, 183–197.

Capovilla, M., Brandt, M., and Botas, J. (1994). Direct regulation of *decapentaplegic* by *Ultrabithorax* and its role in Drosophila midgut morphogenesis. Cell *76*, 461–475.

Chan, S.-K., and Mann, R. S. (1993). The segment identity functions of Ultrabithorax are contained within its homeodomain and carboxy-terminal sequences. Genes Dev. *7*, 796–811.

Chien, C.-T., Bartel, P., Sternglanz, R., and Fields, S. (1991). The two-hybrid system: a method to identify and clone genes for proteins that interact with a protein of interest. Proc. Natl. Acad. Sci. USA *88*, 9578–9582.

Desplan, C., Theis, J., and O'Farrell, P. H. (1988). The sequence specificity of homeodomain–DNA interaction. Cell *54*, 1081–1090.

Dessain, S., Gross, C. T., Kuziora, M. A., and McGinnis, W. (1992). Antp-type homeodomains have distinct DNA binding specificities that correlate with their different regulatory functions in embryos. EMBO J. *11*, 991–1002.

Durfee, T., Becherer, K., Chen, P.-L., Yeh, S.-H., Yang, Y., Kilburn, A. E., Lee, W.-H., and Elledge, S. J. (1993). The retinoblastoma protein associates with the protein phosphatase type I catalytic subunit. Genes Dev. *7*, 555–569.

Ekker, S., von Kessler, D., and Beachy, P. (1992). Differential DNA sequence recognition is a determinant of specificity in homeotic gene action. EMBO J. *11*, 4059–4072.

Flegel, W. A., Singson, A. W., Margolis, J. S., Bang, A. G., Posakony, J. W., and Murre, C. (1993). *Dpbx*, a new homeobox gene closely related to the human proto-oncogene *pbx1* molecular structure and developmental expression. Mech. Dev. *41*, 155–161.

Furukubo-Tokunaga, K., Flister, S., and Gehring, W. J. (1993). Functional specificity of the Antennapedia homeodomain. Proc. Natl. Acad. Sci USA *90*, 6360–6364.

Gibson, G., and Gehring, W. J. (1988). Head and thoracic transformation caused by ectopic expression of *Antennapedia* during *Drosophila* development. Development *102*, 657–675.

Gonzalez-Reyes, A., and Morata, G. (1990). The developmental effect of overexpressing a *Ubx* product in Drosophila embryos is dependent on its interactions with other homeotic products. Cell *61*, 515–522.

Gonzalez-Reyes, A., Urquia, N., Gehring, W. J., Struhl, G., and Morata, G. (1990). Are cross-regulatory interactions between homoeotic genes functionally significant? Nature *344*, 78–80.

Grueneberg, D., Natesan, S., Alexandre, C., and Gilman, M. Z. (1992). Human and Drosophila homeodomain proteins that enhance the DNA-binding activity of serum response factor. Science *257*, 1089–1095.

Hayashi, S., and Scott, M. P. (1990). What determines the specificity of action of Drosophila homeodomain proteins? Cell *63*, 883–894.

Hoey, T., and Levine, M. (1988). Divergent homeobox proteins recognize similar DNA sequences in *Drosophila*. Nature *332*, 858–861.

Immergluck, K., Lawrence, P. A., and Bienz, M. (1990). Induction across germ layers in Drosophila mediated by a genetic cascade. Cell *62*, 261–268.

Johnson, A. (1993). A combinatorial regulatory circuit in budding yeast. In Transcriptional Regulation, K. Yamamoto and S. McKnight, eds. (Cold Spring Harbor, New York: Cold Spring Harbor Laboratory Press).

Kaelin, W. G., Krek, W., Sellers, W., DeCaprio, J., Ajchenbaum, F., Fuchs, C., Chittenden, T., Li, Y., Farnham, P., Blanar, M., Livingston, D., Flemington, E. (1992). Expression cloning of a cDNA encoding a retinoblastoma-binding protein with E2F-like properties. Cell *70*, 351–364.

Kamps, M. P., Murre, C., Sun, X.-h., and Baltimore, D. (1990). A new homeobox gene contributes the DNA binding domain of the t(1;19) translocation protein in pre-B ALL. Cell *60*, 547–555.

Keleher, C. A., Goutte, C., and Johnson, A. D. (1988). The yeast cell-type-specific repressor α2 acts cooperatively with a non-cell-type-specific protein. Cell *53*, 927–936.

Kissinger, C. R., Liu, B., Martin-Blanco, E., Kornberg, T. B., and Pabo, C. O. (1990). Crystal structure of an engrailed homeodomain–DNA complex at 2.8 A resolution: a framework for understanding homeodomain–DNA interactions. Cell *63*, 579–590.

Lewis, E. B. (1978). A gene complex controlling segmentation in *Drosophila*. Nature *276*, 565–570.

Lin, L., and McGinnis, W. (1992). Mapping functional specificity in the Dfd and Ubx homeodomains. Genes Dev. *6*, 1071–1081.

Lopez, A. J., and Hogness, D. S. (1991). Immunochemical dissection of the *Ultrabithorax* homeoprotein family in *Drosophila melanogaster*. Proc. Natl. Acad. Sci. USA *88*, 9924–9928.

Luban, J., Bossolt, K. L., Franke, E. K., Kalpana, G. V., and Goff, S. P. (1993). Human immunodeficiency virus type I Gag protein binds to Cyclophilins A and Ab. Cell *73*, 1067–1078.